

Supplementary materials for “**Transformation and differential abundance analysis of microbiome data incorporating phylogeny**”

Chao Zhou^{1,3}, Hongyu Zhao^{2,3,*}, and Tao Wang^{1,3,4,*}

¹Department of Bioinformatics and Biostatistics, Shanghai Jiao Tong University

²Department of Biostatistics, Yale University

³SJTU-Yale Joint Center for Biostatistics and Data Science, Shanghai Jiao Tong University

⁴MoE Key Lab of Artificial Intelligence, Shanghai Jiao Tong University

*Corresponding author: hongyu.zhao@yale.edu; neowangtao@sjtu.edu.cn

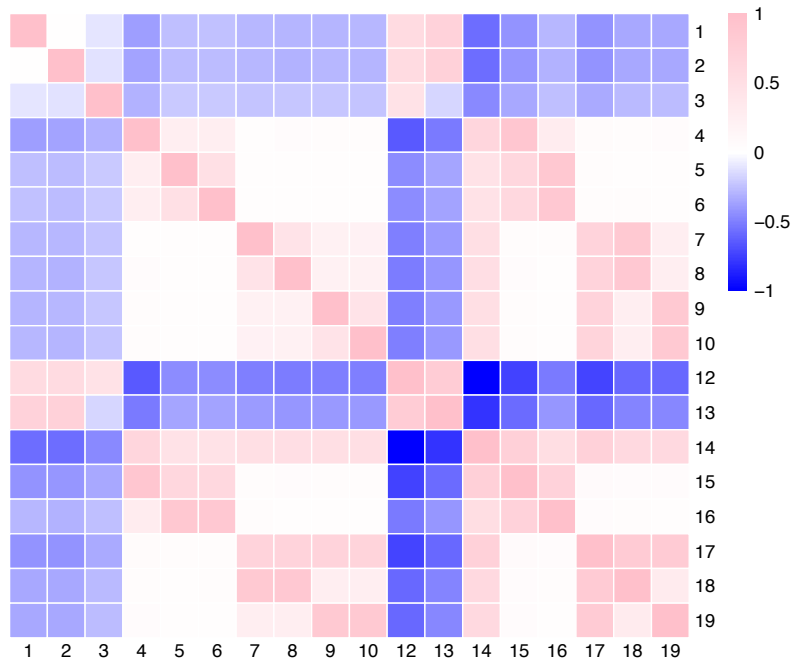


Figure S1. The sample correlations among counts on the tree in Figure 1 when the underlying distribution is DTM.

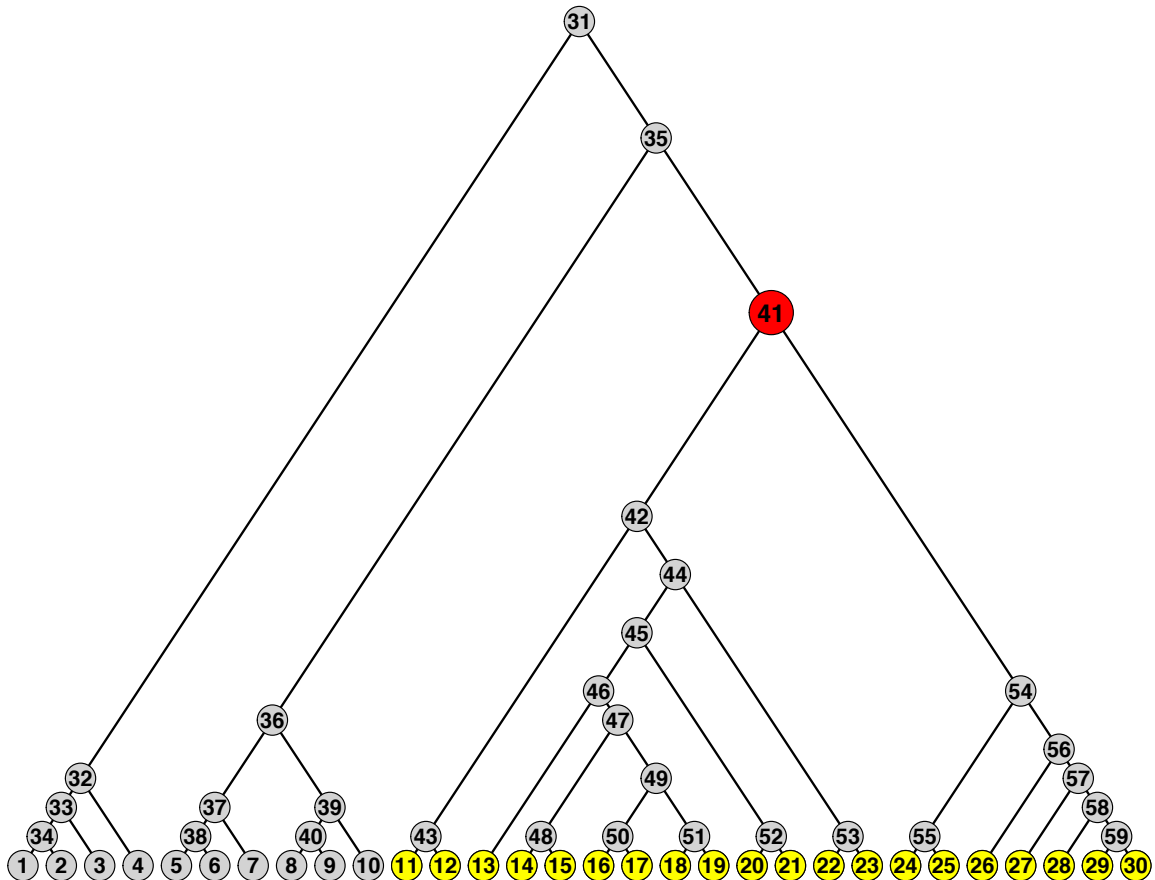


Figure S2. A binary tree with $K = 30$. The internal node 41 (red) and the corresponding leaves (yellow) were set to be differentially abundant (DA) between two groups.

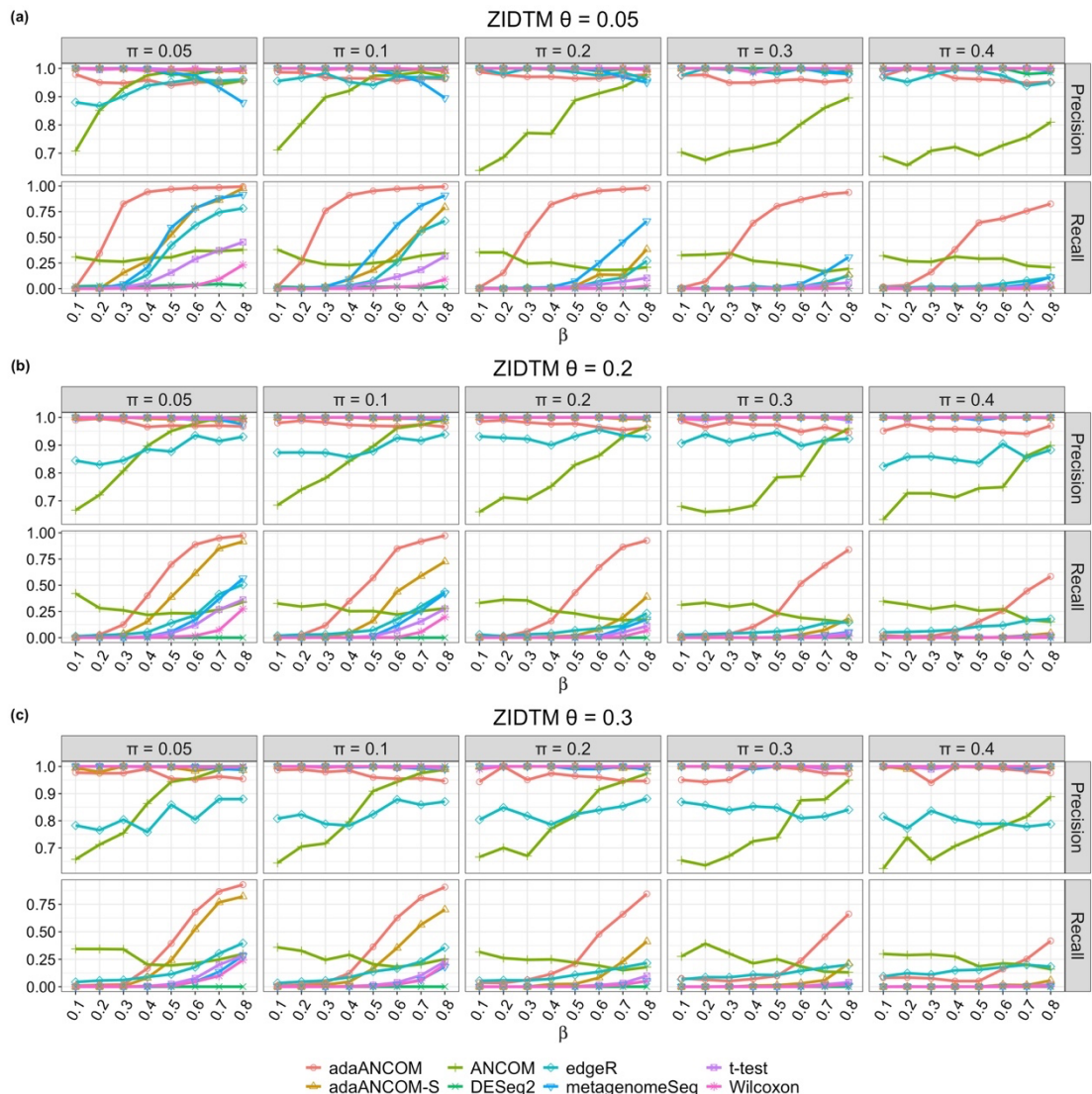


Figure S3. Precision and recall comparison of different DA testing methods. (a) Data were generated from ZIDTM with varying values of zero-inflation proportion $\pi_v = \pi$ and a fixed dispersion $\theta_v = \theta = 0.05$, with the tree and DA pattern depicted in Figure S2; (b) Data were generated in the same way as in (a), except that $\theta = 0.2$; (c) Data were generated in the same way as in (a), except that $\theta = 0.3$.

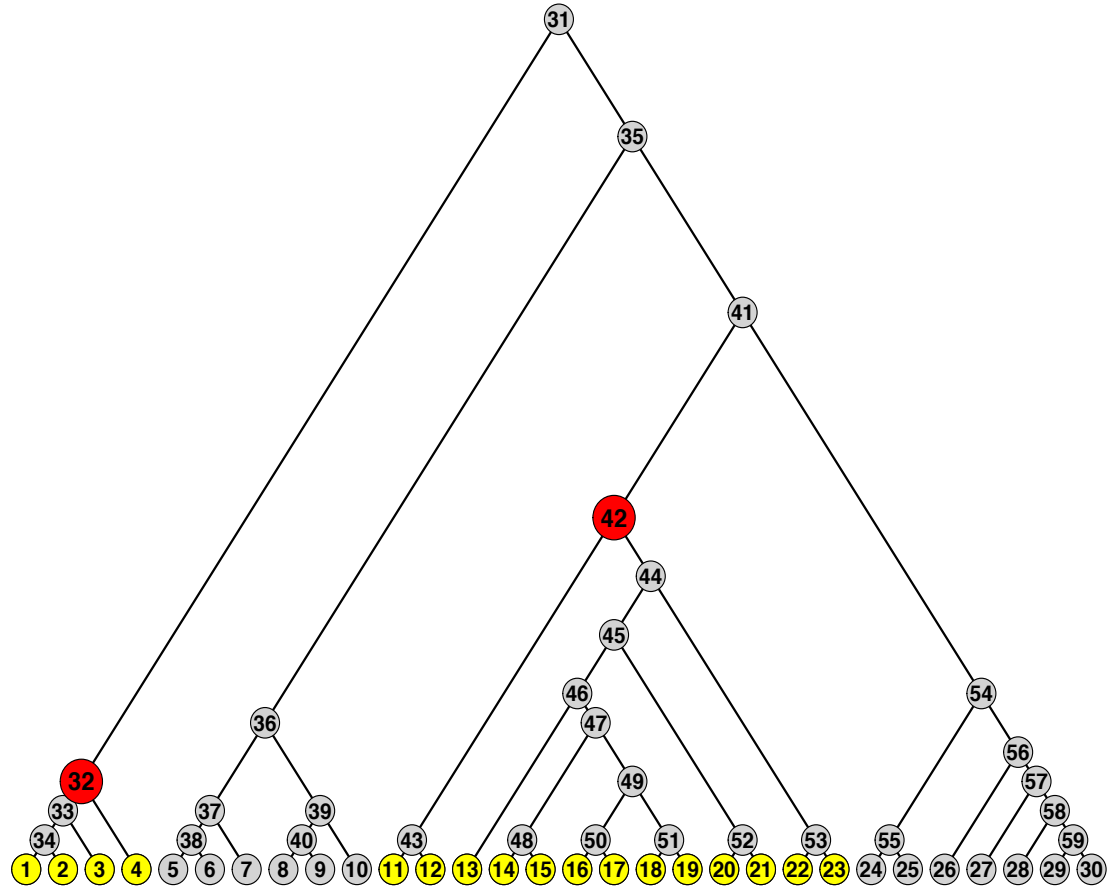


Figure S4. The same binary tree as in Figure S2, except that two internal nodes 32 and 42 (red), and the corresponding leaves (yellow) were set to be DA between two groups.

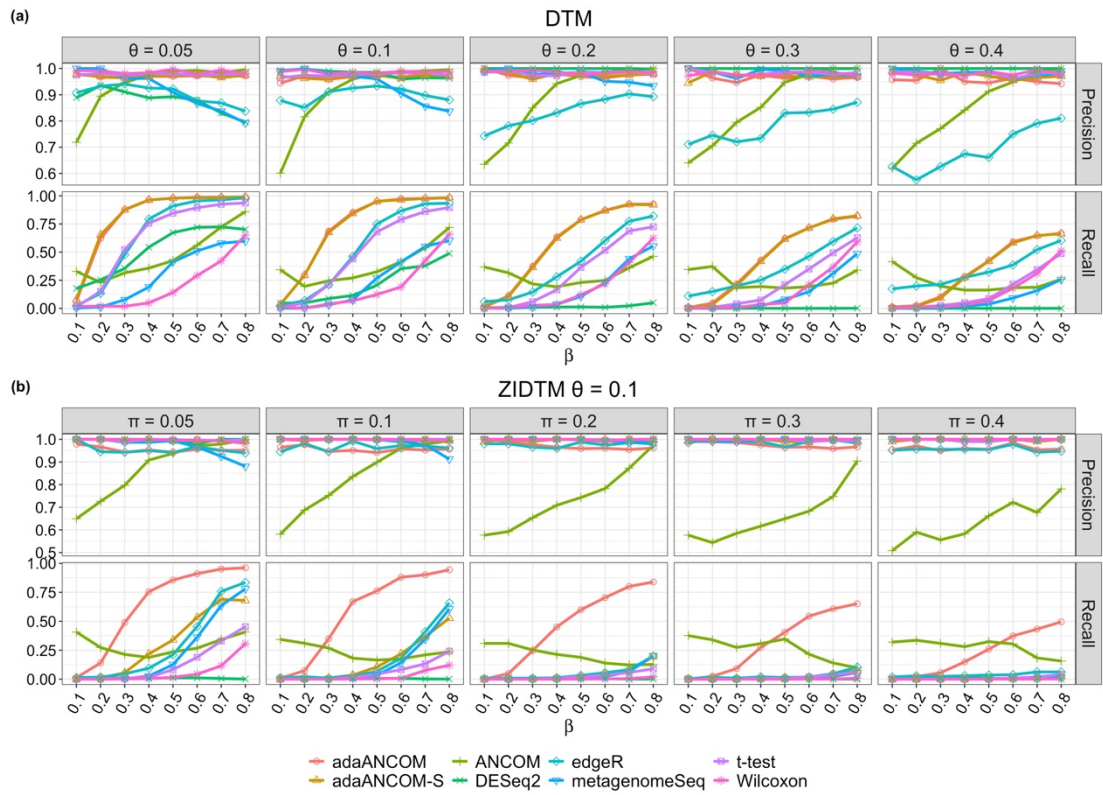


Figure S5. Precision and recall comparison of different DA testing methods. (a) Data were generated from DTM with varying values of dispersion parameter $\theta_v = \theta$ and effect size β , with the tree and DA pattern depicted in Figure S4; (b) Data were generated from ZIDTM with varying values of zero-inflation proportion $\pi_v = \pi$ and a fixed dispersion $\theta_v = \theta = 0.1$, with the tree and DA pattern depicted in Figure S4.

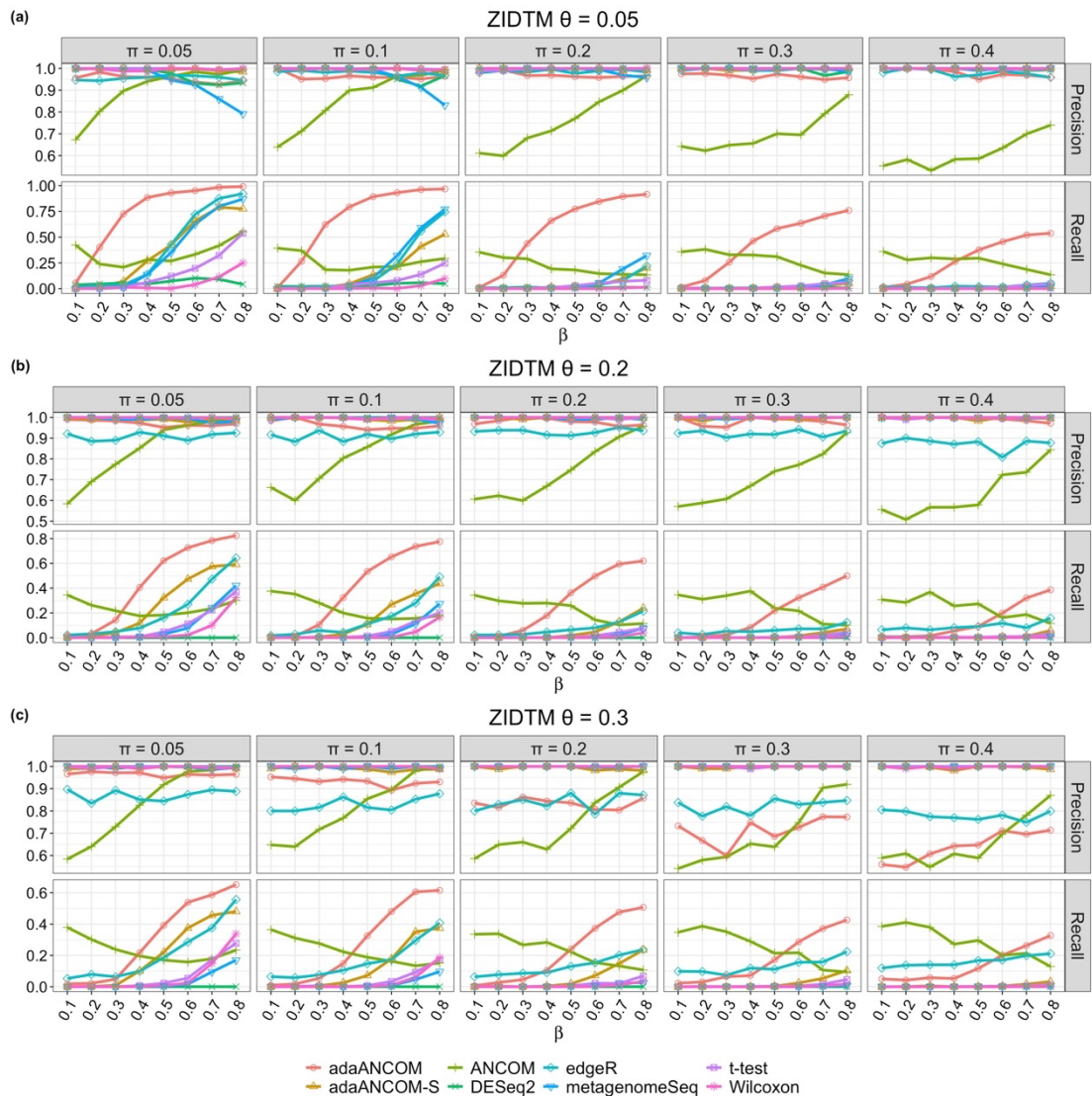


Figure S6. Precision and recall comparison of different DA testing methods. (a) Data were generated from ZIDTM with varying values of zero-inflation proportion $\pi_v = \pi$ and a fixed dispersion $\theta_v = \theta = 0.05$, with the tree and DA pattern depicted in Figure S4; (b) Data were generated in the same way as in (a), except that $\theta = 0.2$; (c) Data were generated in the same way as in (a), except that $\theta = 0.3$.

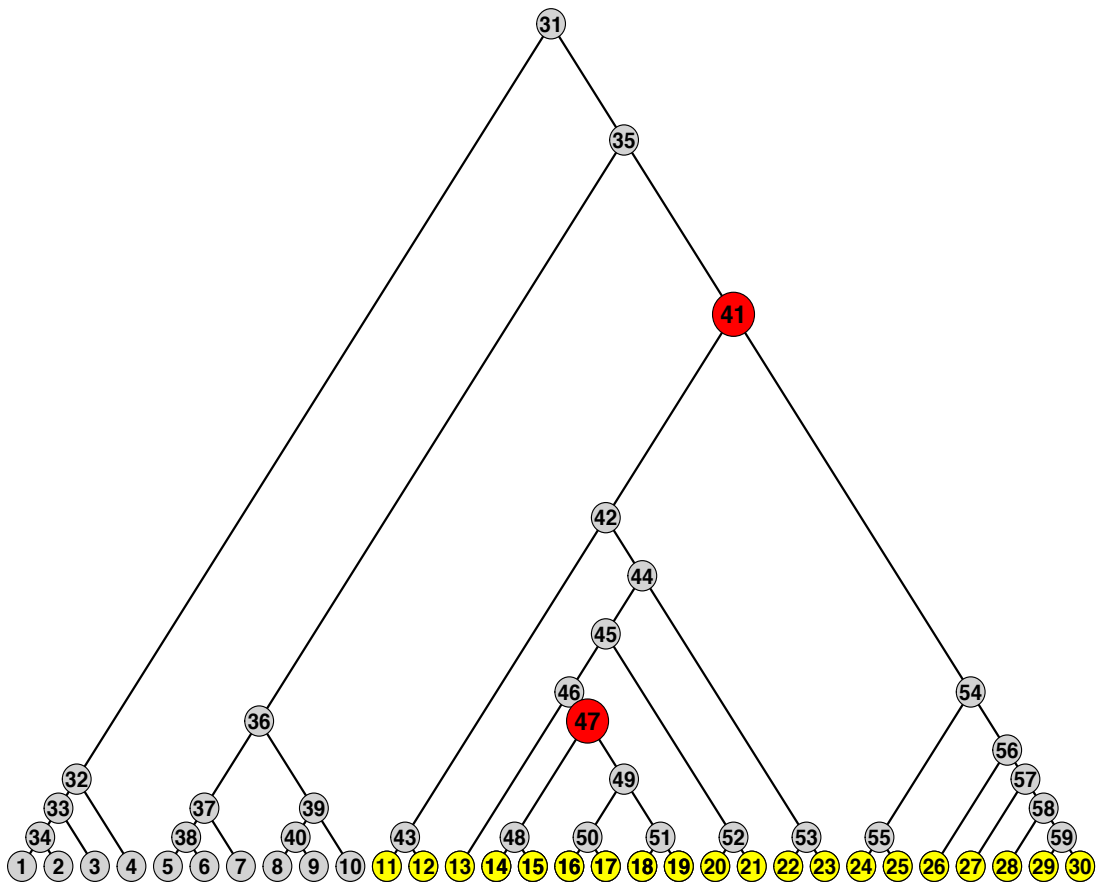


Figure S7. The same binary tree as in Figures S2 and S4, except that two nested internal nodes 41 and 47 (red), and the corresponding leaves (yellow) were set to be DA between two groups.

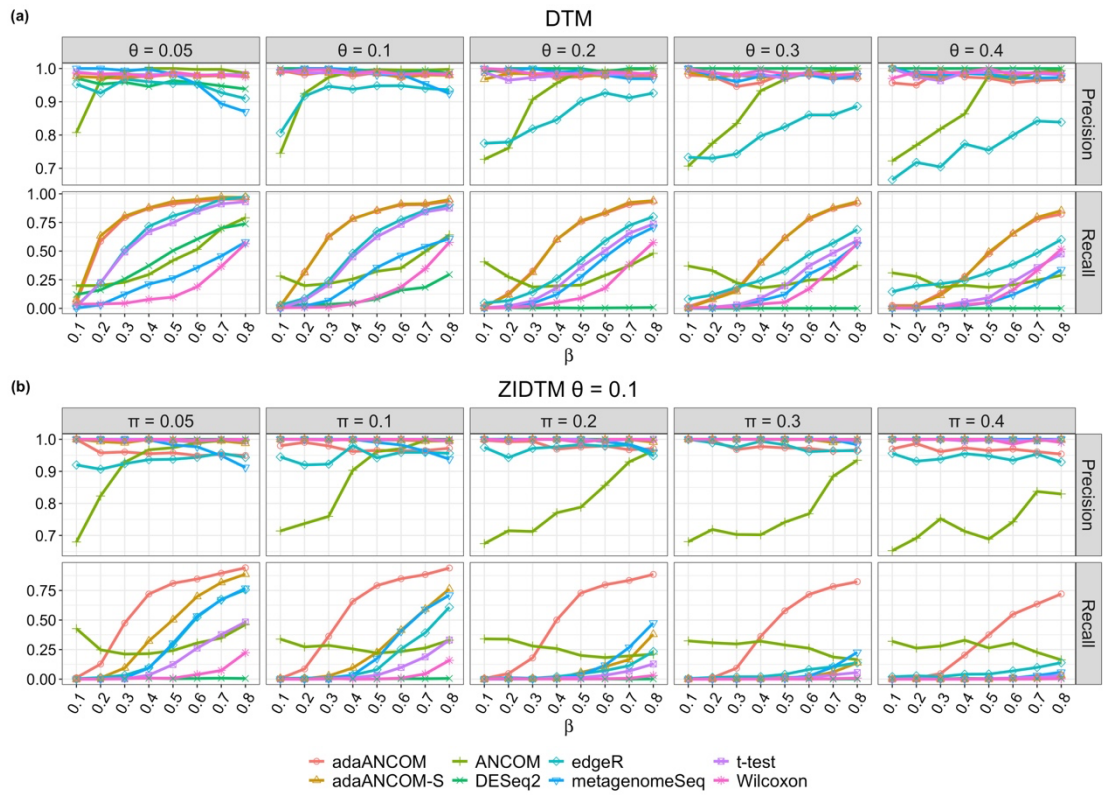


Figure S8. Precision and recall comparison of different DA testing methods. (a) Data were generated from DTM with varying values of dispersion parameter $\theta_v = \theta$ and effect size β , with the tree and DA pattern depicted in Figure S7; (b) Data were generated from ZIDTM with varying values of zero-inflation proportion $\pi_v = \pi$ and a fixed dispersion $\theta_v = \theta = 0.1$, with the tree and DA pattern depicted in Figure S7.

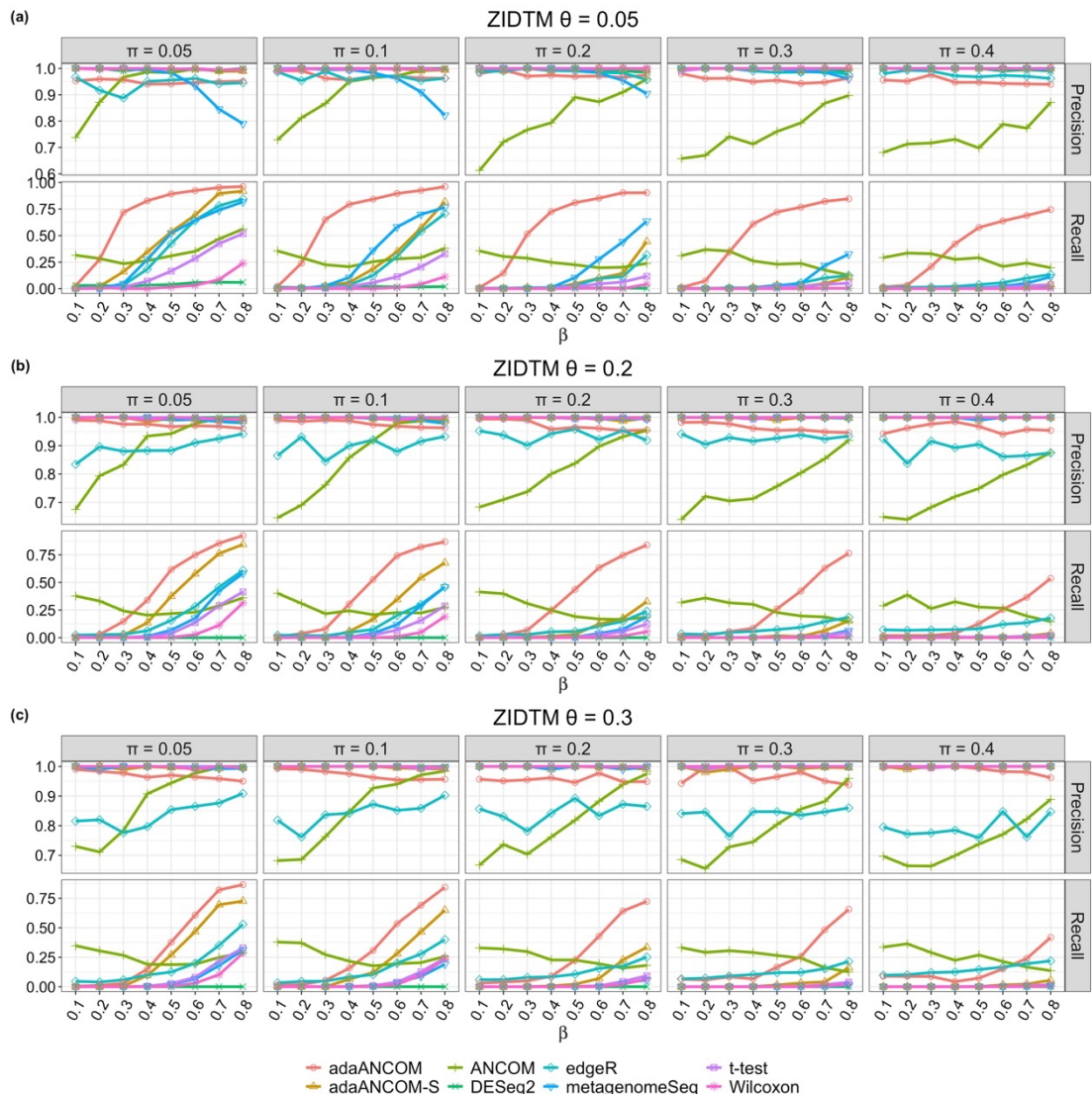


Figure S9. Precision and recall comparison of different DA testing methods. (a) Data were generated from ZIDTM with varying values of zero-inflation proportion $\pi_v = \pi$ and a fixed dispersion $\theta_v = \theta = 0.05$, with the tree and DA pattern depicted in Figure S7; (b) Data were generated in the same way as in (a), except that $\theta = 0.2$; (c) Data were generated in the same way as in (a), except that $\theta = 0.3$.

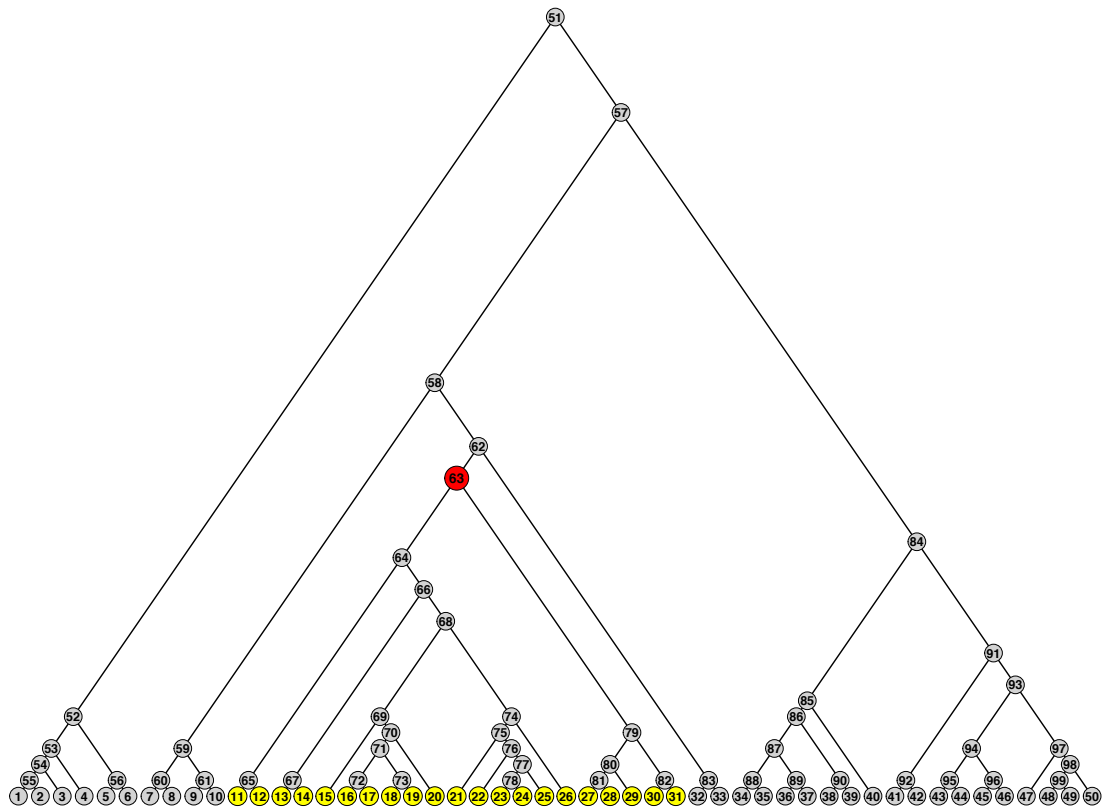


Figure S10. A binary tree with $K = 50$. The internal node 63 (red) and the corresponding leaves (yellow) were set to be DA between two groups. The number of the DA leaves is comparable to those in Figures S2, S4, and S7.

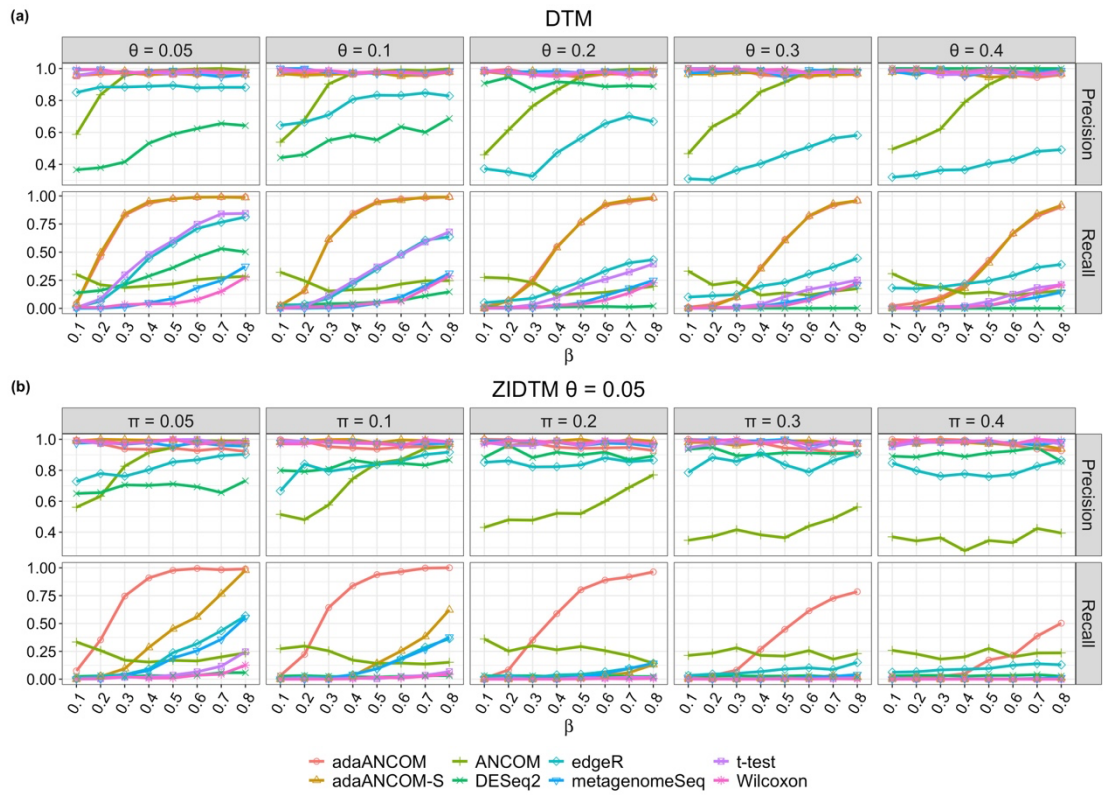


Figure S11. Precision and recall comparison of different DA testing methods. (a) Data were generated from DTM with varying values of dispersion parameter $\theta_v = \theta$ and effect size β , with the tree and DA pattern depicted in Figure S10; (b) Data were generated from ZIDTM with varying values of zero-inflation proportion $\pi_v = \pi$ and a fixed dispersion $\theta_v = \theta = 0.05$, with the tree and DA pattern depicted in Figure S10.

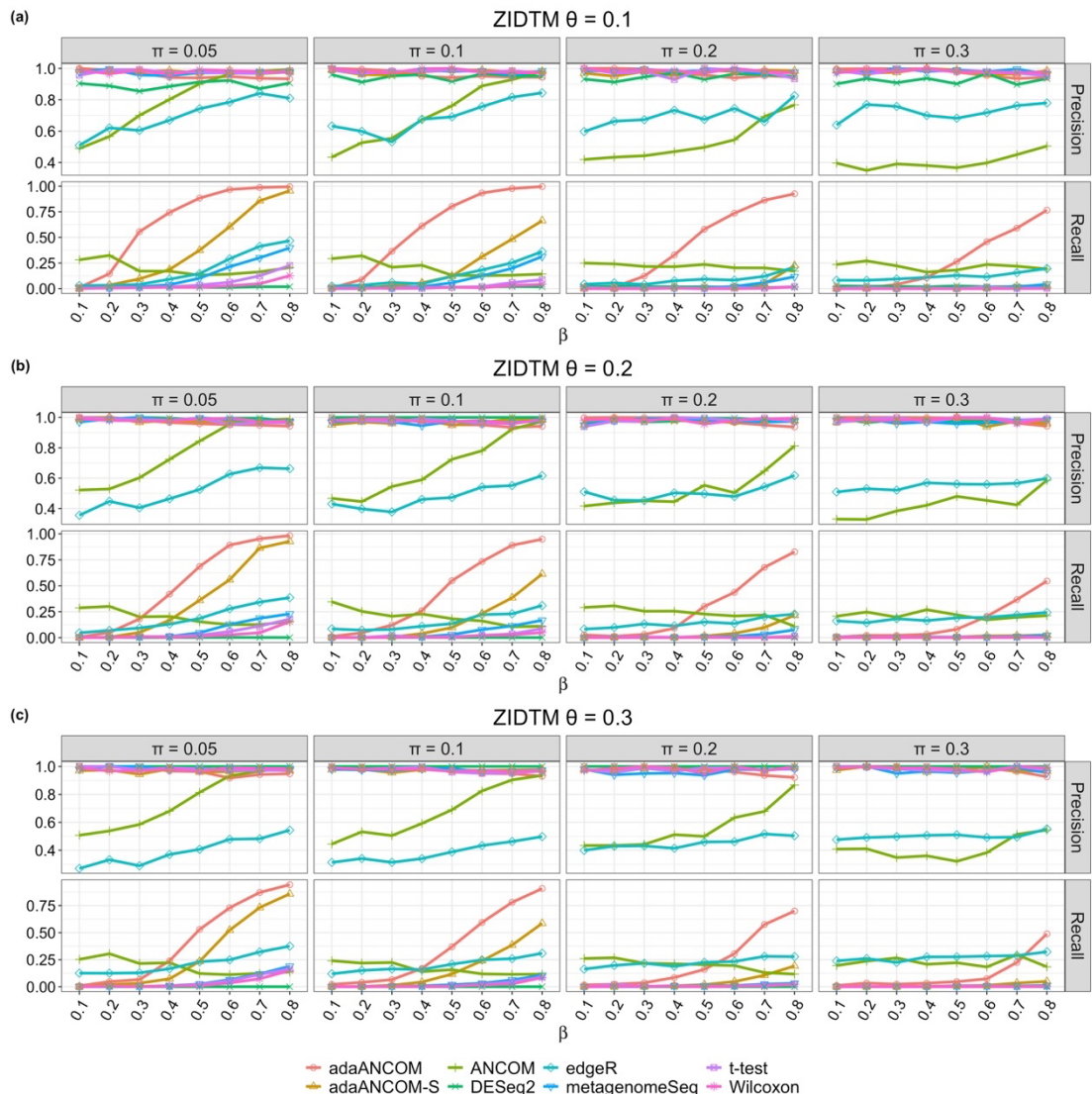


Figure S12. Precision and recall comparison of different DA testing methods. (a) Data were generated from ZIDTM with varying values of zero-inflation proportion $\pi_v = \pi$ and a fixed dispersion $\theta_v = \theta = 0.1$, with the tree and DA pattern depicted in Figure S10; (b) Data were generated in the same way as in (a), except that $\theta = 0.2$; (c) Data were generated in the same way as in (a), except that $\theta = 0.3$.

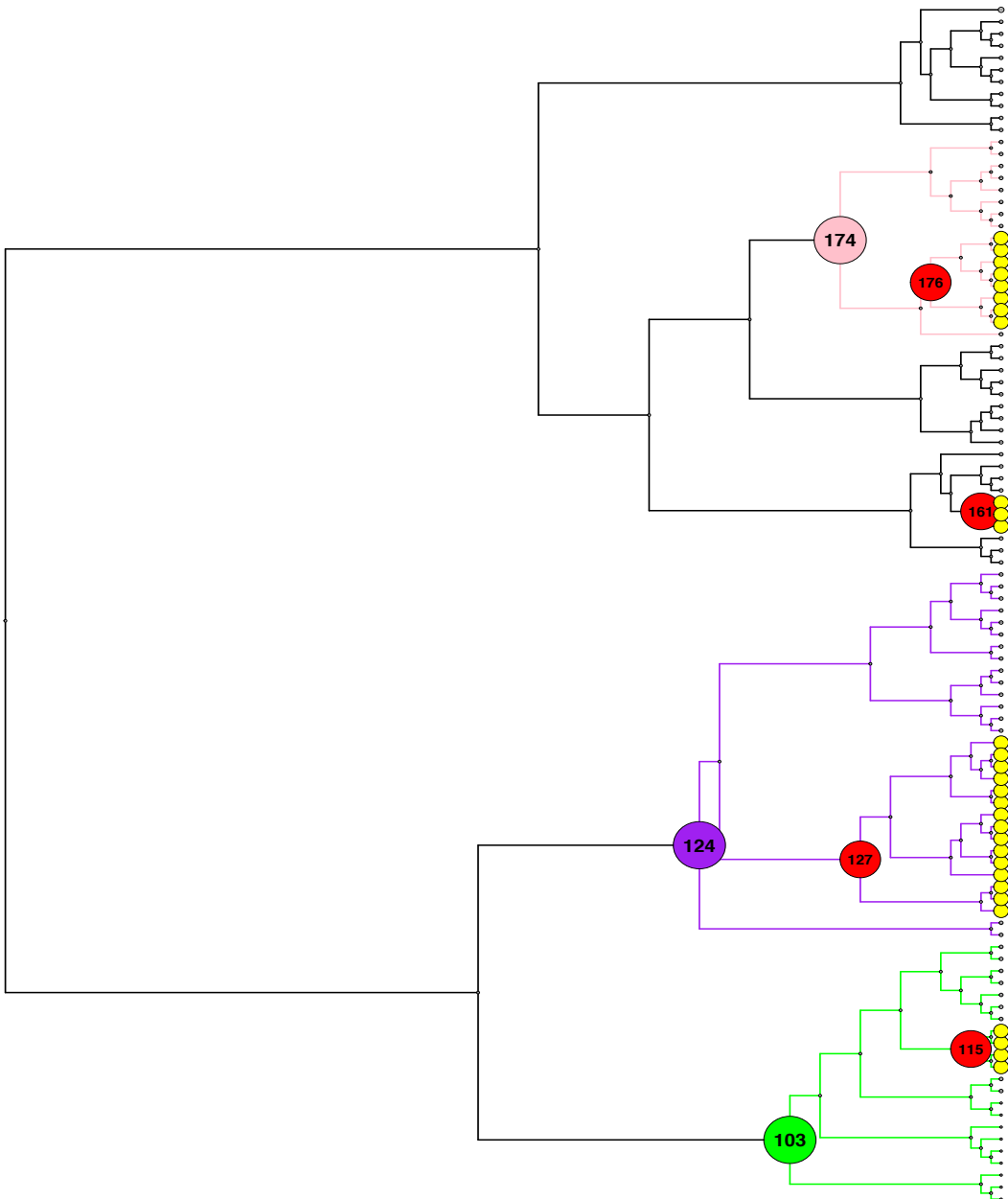


Figure S13. A binary tree with $K = 100$. DA internal nodes are shown in red and DA leaves are shown in yellow. Three subtrees, indexed by the internal nodes 103, 124, and 174, are depicted in green, blue, and pink, respectively. Data were generated from ZIDTM with parameters learned based on the HMP data, as detailed in the next figure.

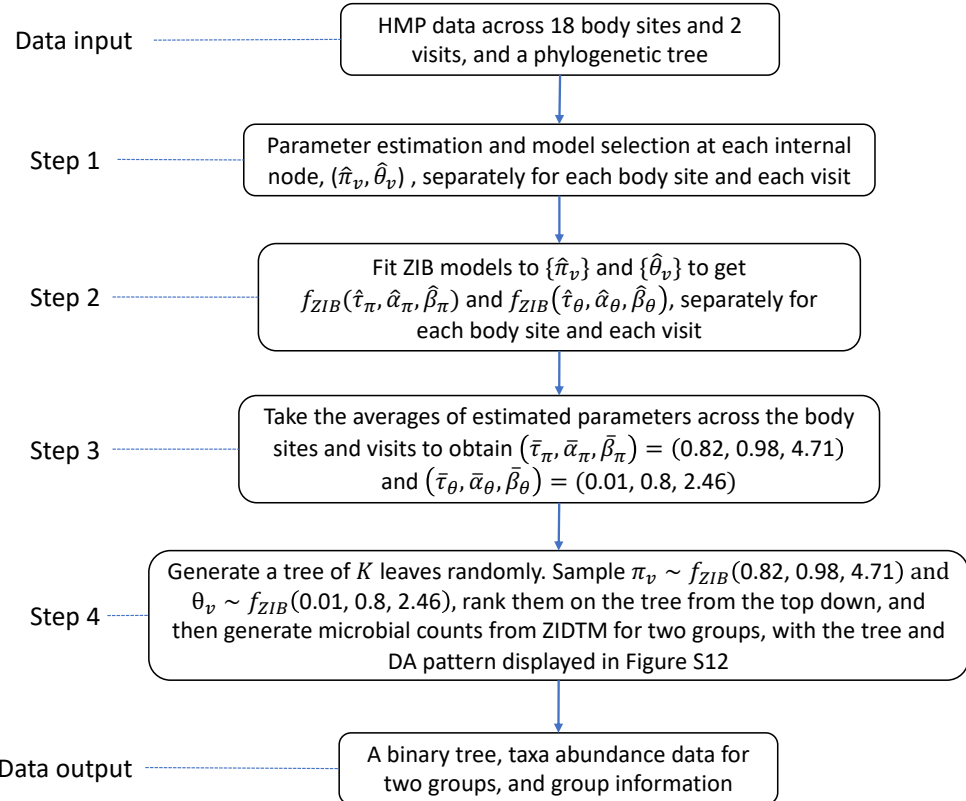


Figure S14. Data generation process. Taxa abundance data were generated from ZIDTM with parameters estimated based on HMP data. Here τ represents the probability of zero-inflation in the ZIB model. This is to be distinguished from π in zero-inflated models of the main text.

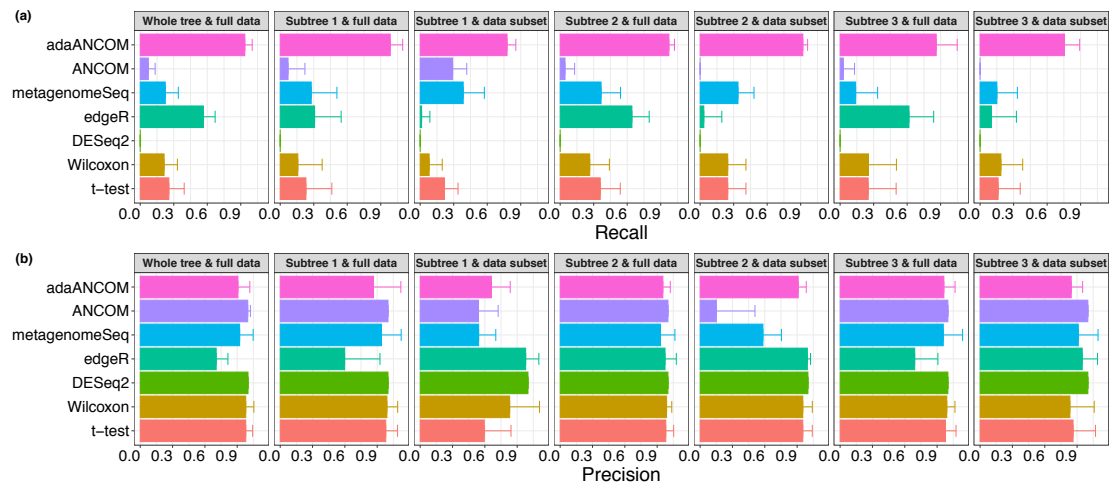


Figure S15. Recall and precision comparison of different DA testing methods. Data were generated from ZIDTM with parameters estimated based on the HMP data, and with the tree and DA pattern depicted in Figure S13. adaANCOM had the highest recall and comparable precision with other methods across all scenarios.

| | Methods | DTM | | | ZIDTM | | |
|-----------|---------------|--------|-----------|--------|--------|-----------|--------|
| | | Recall | Precision | F1 | Recall | Precision | F1 |
| Setting 1 | t-test | 0.9460 | 0.6541 | 0.7734 | 0.6120 | 0.6263 | 0.6137 |
| | | 0.0243 | 0.0065 | 0.0130 | 0.1117 | 0.0672 | 0.0670 |
| | Wilcoxon | 0.8615 | 0.6326 | 0.7295 | 0.8445 | 0.6400 | 0.7274 |
| | | 0.0245 | 0.0064 | 0.0129 | 0.0594 | 0.0243 | 0.0319 |
| | metagenomeSeq | 0.7085 | 0.9879 | 0.8243 | 0.7990 | 0.6505 | 0.7164 |
| | | 0.0356 | 0.0351 | 0.0234 | 0.0678 | 0.0278 | 0.0407 |
| | ANCOM | 0.7390 | 0.9994 | 0.8489 | 0.3571 | 0.8764 | 0.5068 |
| | | 0.0430 | 0.0059 | 0.0307 | 0.0456 | 0.0609 | 0.0503 |
| | DESeq2 | 0.8460 | 0.6605 | 0.7132 | 0.1295 | 1.0000 | 0.1768 |
| | | 0.1845 | 0.0877 | 0.1493 | 0.2099 | 0.0000 | 0.2857 |
| Setting 2 | edgeR | 0.8915 | 0.6515 | 0.7513 | 0.8340 | 0.7490 | 0.7767 |
| | | 0.0310 | 0.0528 | 0.0266 | 0.0791 | 0.1453 | 0.0581 |
| | adaANCOM-S | 0.9500 | 0.9595 | 0.9546 | 0.8335 | 0.9868 | 0.9017 |
| | | 0.0174 | 0.0207 | 0.0138 | 0.0772 | 0.0245 | 0.0473 |
| | adaANCOM | 0.9505 | 1.0000 | 0.9745 | 0.9410 | 1.0000 | 0.9672 |
| | | 0.0181 | 0.0000 | 0.0098 | 0.0911 | 0.0000 | 0.0522 |
| | t-test | 0.9300 | 0.5489 | 0.6903 | 0.6812 | 0.5031 | 0.5775 |
| | | 0.0232 | 0.0067 | 0.0116 | 0.0680 | 0.0367 | 0.0413 |
| | Wilcoxon | 0.8765 | 0.5340 | 0.6636 | 0.6935 | 0.4776 | 0.5655 |
| | | 0.0177 | 0.0052 | 0.0091 | 0.0497 | 0.0201 | 0.0303 |
| | metagenomeSeq | 0.6265 | 0.8073 | 0.7010 | 0.8553 | 0.5762 | 0.6878 |
| | | 0.0676 | 0.0817 | 0.0498 | 0.0505 | 0.0342 | 0.0342 |
| Setting 2 | ANCOM | 0.7291 | 0.7971 | 0.7595 | 0.6714 | 0.8044 | 0.7302 |
| | | 0.0650 | 0.0410 | 0.0387 | 0.0544 | 0.0952 | 0.0565 |
| | DESeq2 | 0.9106 | 0.5831 | 0.6869 | 0.1194 | 0.9293 | 0.1193 |
| | | 0.1895 | 0.0764 | 0.0872 | 0.2489 | 0.1474 | 0.2482 |
| | edgeR | 0.8776 | 0.5425 | 0.6702 | 0.8953 | 0.6137 | 0.7247 |
| | | 0.0492 | 0.0160 | 0.0237 | 0.0477 | 0.0927 | 0.0675 |
| | adaANCOM-S | 0.9194 | 0.9939 | 0.9541 | 0.5824 | 0.9764 | 0.7270 |
| | | 0.0546 | 0.0175 | 0.0255 | 0.0717 | 0.0414 | 0.0587 |
| | adaANCOM | 0.9194 | 0.9983 | 0.9564 | 0.7859 | 0.9704 | 0.8662 |
| | | 0.0546 | 0.0122 | 0.0290 | 0.0682 | 0.0478 | 0.0423 |

Table S1. Recall, precision, and F1 comparison of different DA testing methods. Initially, data were generated from DTM ($\theta_v = \theta = 0.1$) or ZIDTM ($\theta_v = \theta = \pi_v = \pi = 0.1$) with the same parameters for the two groups, and tree depicted in Figure S2. Then we multiplied the counts for leaf nodes in yellow depicted in Figure S2 (Setting 1) and Figure S4 (Setting 2) by some effect size for one group. The log effect size was drawn uniformly from -5 to 5 . Each method has associated with it two rows showing respectively the mean and standard error over 100 replicates.

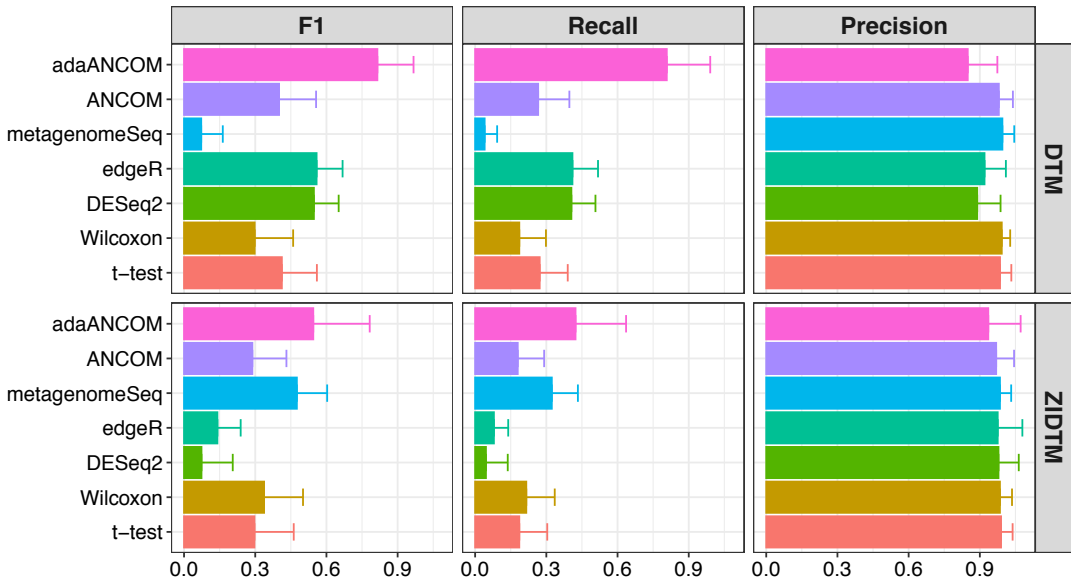


Figure S16. Recall, precision, and F1 comparison of different DA testing methods. Data were generated from SparseDOSSA 2 with parameters estimated based on synthetic DTM ($\theta_v = \theta = 0.1$) and ZIDTM ($\theta_v = \theta = \pi_v = \pi = 0.1$) data, and with the tree and DA pattern depicted in Figure S2. adaANCOM had the highest recall and comparable precision with other methods across both scenarios.

| Body site | Sample size | Species | Genus | Family | Order | Class | Phylum |
|-------------------------------------|--------------------|----------------|--------------|---------------|--------------|--------------|---------------|
| <i>Anterior_nares</i> | 77 | 612 | 35 | 32 | 16 | 12 | 8 |
| | | 0.60 | 0.47 | 0.41 | 0.35 | 0.35 | 0.35 |
| <i>Attached_Keratinized_gingiva</i> | 104 | 881 | 39 | 29 | 16 | 11 | 7 |
| | | 0.63 | 0.40 | 0.35 | 0.23 | 0.11 | 0.15 |
| <i>Buccal_mucosa</i> | 104 | 1221 | 47 | 35 | 19 | 13 | 9 |
| | | 0.62 | 0.36 | 0.33 | 0.22 | 0.15 | 0.19 |
| <i>Hard_palate</i> | 99 | 1244 | 49 | 35 | 18 | 14 | 9 |
| | | 0.61 | 0.32 | 0.26 | 0.15 | 0.16 | 0.15 |
| <i>Left_Antecubital_fossa</i> | 60 | 341 | 33 | 37 | 16 | 12 | 6 |
| | | 0.62 | 0.55 | 0.52 | 0.41 | 0.38 | 0.25 |
| <i>Left_Retroauricular_cresce</i> | 105 | 489 | 23 | 25 | 12 | 8 | 6 |
| | | 0.58 | 0.52 | 0.49 | 0.37 | 0.28 | 0.30 |
| <i>Mid_vagina</i> | 52 | 430 | 26 | 26 | 14 | 10 | 5 |
| | | 0.65 | 0.57 | 0.53 | 0.43 | 0.33 | 0.16 |
| <i>Palatine_Tonsils</i> | 108 | 1289 | 56 | 37 | 21 | 15 | 10 |
| | | 0.61 | 0.32 | 0.26 | 0.20 | 0.14 | 0.14 |
| <i>Posterior_fornix</i> | 53 | 388 | 18 | 21 | 11 | 8 | 5 |
| | | 0.64 | 0.63 | 0.61 | 0.48 | 0.34 | 0.25 |
| <i>Right_Antecubital_fossa</i> | 63 | 348 | 35 | 33 | 16 | 11 | 6 |
| | | 0.61 | 0.55 | 0.47 | 0.39 | 0.36 | 0.25 |
| <i>Right_Retroauricular_cresce</i> | 107 | 440 | 21 | 24 | 12 | 8 | 5 |
| | | 0.59 | 0.54 | 0.52 | 0.41 | 0.32 | 0.23 |
| <i>Saliva</i> | 79 | 1130 | 56 | 40 | 21 | 14 | 9 |
| | | 0.61 | 0.35 | 0.30 | 0.21 | 0.12 | 0.10 |
| <i>Stool</i> | 108 | 1036 | 49 | 23 | 13 | 10 | 6 |
| | | 0.65 | 0.38 | 0.36 | 0.44 | 0.32 | 0.15 |
| <i>Subgingival_plaque</i> | 104 | 1199 | 50 | 40 | 22 | 15 | 10 |
| | | 0.63 | 0.32 | 0.33 | 0.27 | 0.18 | 0.20 |
| <i>Supragingival_plaque</i> | 108 | 1248 | 42 | 32 | 18 | 14 | 9 |
| | | 0.61 | 0.29 | 0.28 | 0.21 | 0.20 | 0.19 |
| <i>Throat</i> | 90 | 1105 | 52 | 39 | 21 | 14 | 9 |
| | | 0.60 | 0.34 | 0.32 | 0.21 | 0.12 | 0.11 |
| <i>Tongue_dorsum</i> | 112 | 1513 | 43 | 33 | 19 | 14 | 9 |
| | | 0.60 | 0.28 | 0.27 | 0.20 | 0.14 | 0.14 |
| <i>Vaginal_introitus</i> | 52 | 465 | 30 | 28 | 14 | 10 | 5 |
| | | 0.65 | 0.52 | 0.50 | 0.41 | 0.32 | 0.14 |

Table S2. Information on the preprocessed HMP data. Each body site has associated with it two rows showing respectively taxon number and zero proportion at different taxonomic levels.

| Body site | Visit | Species | Genus | Family | Order | Class | Phylum |
|--|--------------|----------------|--------------|---------------|--------------|--------------|---------------|
| <i>Anterior_nares</i> | 1 | 0.0736 | 0.2059 | 0.1935 | 0.1333 | 0.0909 | 0.2857 |
| | 2 | 0.0690 | 0.1471 | 0.1290 | 0.0667 | 0.0909 | 0.2857 |
| <i>Attached_Keratinized_gingiva</i> | 1 | 0.0676 | 0.0263 | 0.0357 | 0.0000 | 0.0000 | 0.1667 |
| | 2 | 0.0507 | 0.1053 | 0.1071 | 0.0667 | 0.0000 | 0.0000 |
| <i>Buccal_mucosa</i> | 1 | 0.0472 | 0.0870 | 0.0882 | 0.1111 | 0.0000 | 0.0000 |
| | 2 | 0.0552 | 0.0652 | 0.0882 | 0.0556 | 0.0833 | 0.1250 |
| <i>Hard_palate</i> | 1 | 0.0632 | 0.0833 | 0.0882 | 0.1176 | 0.1538 | 0.1250 |
| | 2 | 0.0556 | 0.1458 | 0.1176 | 0.1765 | 0.0769 | 0.2500 |
| <i>Left_Antecubital_fossa</i> | 1 | 0.0902 | 0.3438 | 0.6111 | 0.3333 | 0.4545 | 0.0000 |
| | 2 | 0.0392 | 0.4688 | 0.3333 | 0.3333 | 0.3636 | 0.0000 |
| <i>Left_Retroauricular_cleft_crease</i> | 1 | 0.0802 | 0.0909 | 0.2500 | 0.4545 | 0.4286 | 0.6000 |
| | 2 | 0.0430 | 0.0455 | 0.0417 | 0.0909 | 0.1429 | 0.0000 |
| <i>Mid_vagina</i> | 1 | 0.0427 | 0.0800 | 0.1200 | 0.0000 | 0.0000 | 0.0000 |
| | 2 | 0.0517 | 0.1304 | 0.1600 | 0.1538 | 0.1111 | 0.2500 |
| <i>Palatine_Tonsils</i> | 1 | 0.0722 | 0.0727 | 0.0278 | 0.1000 | 0.0714 | 0.1111 |
| | 2 | 0.0430 | 0.1091 | 0.1111 | 0.1000 | 0.0714 | 0.1111 |
| <i>Posterior_fornix</i> | 1 | 0.0377 | 0.0588 | 0.1000 | 0.0000 | 0.0000 | 0.0000 |
| | 2 | 0.0503 | 0.1176 | 0.1000 | 0.1000 | 0.0000 | 0.0000 |
| <i>Right_Antecubital_fossa</i> | 1 | 0.0646 | 0.4118 | 0.5000 | 0.6000 | 0.4000 | 0.0000 |
| | 2 | 0.0646 | 0.2941 | 0.3438 | 0.2000 | 0.5000 | 0.4000 |
| <i>Right_Retroauricular_cleft_crease</i> | 1 | 0.0868 | 0.1000 | 0.2174 | 0.1818 | 0.2857 | 0.2500 |
| | 2 | 0.0547 | 0.1000 | 0.1739 | 0.1818 | 0.0000 | 0.2500 |
| <i>Saliva</i> | 1 | 0.0826 | 0.3455 | 0.3846 | 0.4000 | 0.2308 | 0.1250 |
| | 2 | 0.0941 | 0.3455 | 0.3077 | 0.4000 | 0.3846 | 0.2500 |
| <i>Stool</i> | 1 | 0.1251 | 0.2292 | 0.2273 | 0.1667 | 0.0000 | 0.0000 |
| | 2 | 0.1275 | 0.1667 | 0.2727 | 0.2500 | 0.2222 | 0.0000 |
| <i>Subgingival_plaque</i> | 1 | 0.0833 | 0.2041 | 0.1538 | 0.1905 | 0.2143 | 0.1111 |
| | 2 | 0.0656 | 0.1429 | 0.1026 | 0.1429 | 0.0714 | 0.3333 |
| <i>Supragingival_plaque</i> | 1 | 0.0721 | 0.0976 | 0.1290 | 0.1176 | 0.0769 | 0.1250 |
| | 2 | 0.0669 | 0.1463 | 0.1613 | 0.1765 | 0.1538 | 0.1250 |
| <i>Throat</i> | 1 | 0.0769 | 0.1961 | 0.1842 | 0.1500 | 0.1538 | 0.1250 |
| | 2 | 0.0553 | 0.0784 | 0.1316 | 0.0500 | 0.0000 | 0.0000 |
| <i>Tongue_dorsum</i> | 1 | 0.0685 | 0.1667 | 0.1250 | 0.1111 | 0.0769 | 0.0000 |
| | 2 | 0.0526 | 0.1190 | 0.1875 | 0.2222 | 0.0769 | 0.1250 |
| <i>Vaginal_introitus</i> | 1 | 0.0421 | 0.0690 | 0.0741 | 0.0000 | 0.0000 | 0.0000 |
| | 2 | 0.0343 | 0.0345 | 0.1111 | 0.0000 | 0.0000 | 0.0000 |

Table S3. The proportions of selecting ZIBB at different taxonomic levels across 18 body sites and 2 visits for the HMP data.

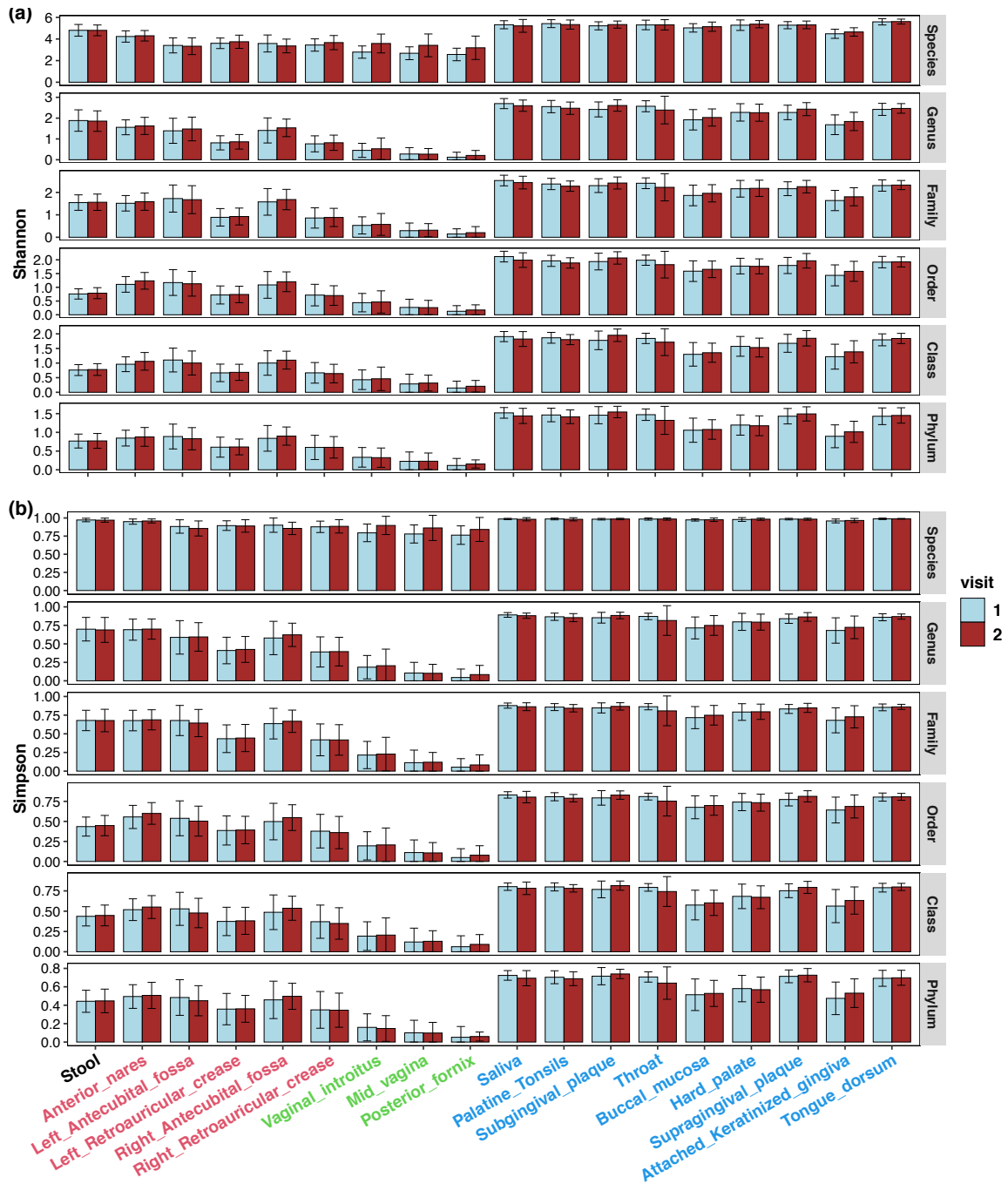


Figure S17. Comparison of Shannon's index and Simpson's index between two visits of each body site across different taxonomic levels. There is no significant difference in alpha diversity after the Bonferroni correction.

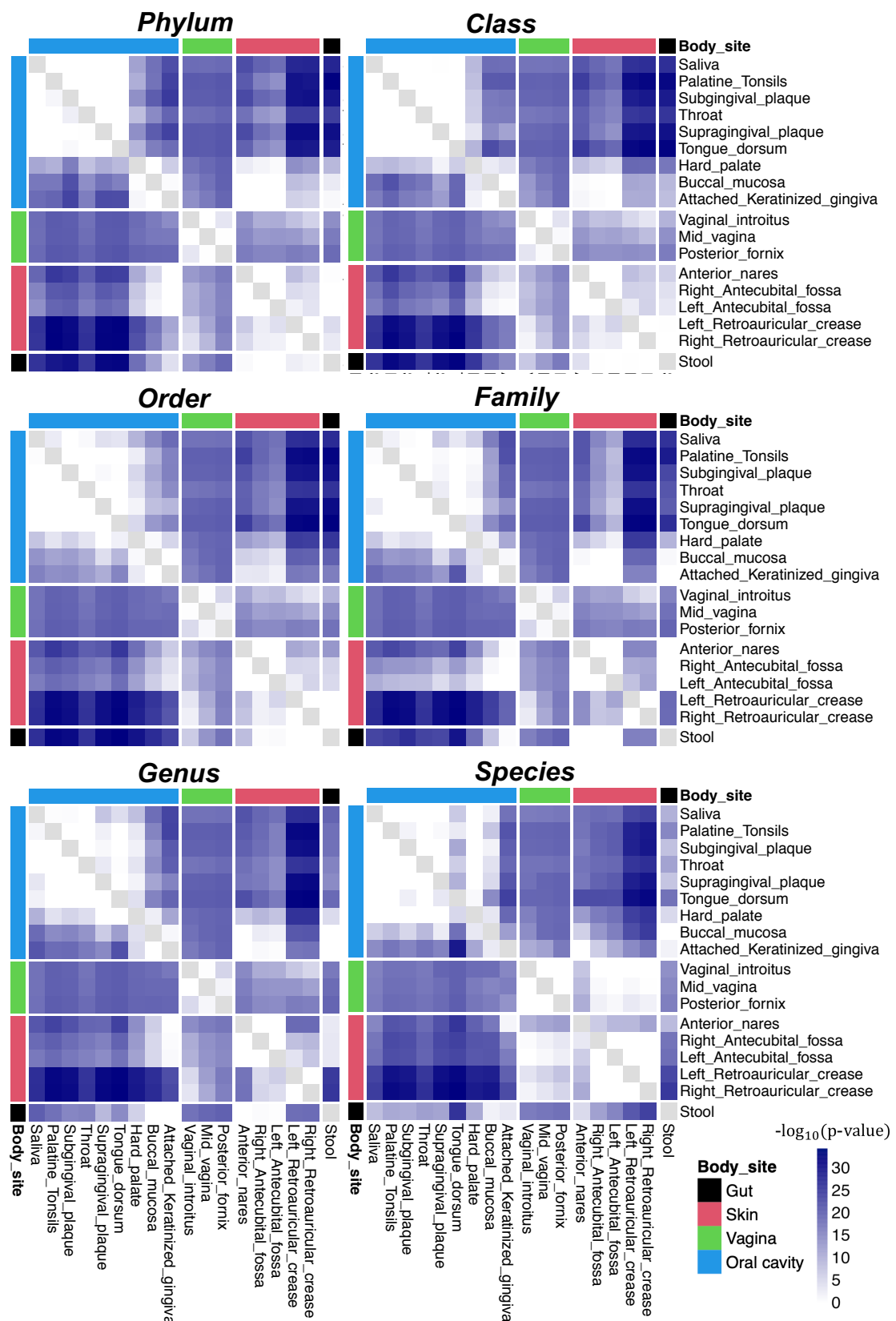


Figure S18. Comparing the alpha diversity between each pair of body sites at different levels. P-values were obtained using the Wilcoxon rank-sum test and Bonferroni correction. The upper and lower triangles show the results for the Shannon's index and the Simpson's index, respectively.

| | t-test | Wilcoxon | ANCOM | metagenomeSeq | edgeR | adaANCOM | adaANCOM-S |
|--------|--------|----------|-------|---------------|-------|----------|------------|
| Before | 69 | 197 | 3 | 192 | 701 | 336 | 271 |
| After | 0 | 0 | 3 | 0 | 17 | 2 | 0 |

Table S4. Numbers of detected species by various methods, before and after multiple testing correction, for HMP stool data between two visits. There were 6965 species of 108 samples for the DA analysis and the zero proportion was about 90%. edgeR stood as an exception, and species detected by it were likely false discoveries. An error occurred for running DESeq2 to estimate the size factor.

| Body site | Species number | t-test | Wilcoxon | ANCOM | MetagenomeSeq | edgeR | ada-ANCOM | ada-ANCOM-S |
|------------------------------|----------------|--------|----------|-------|---------------|-------|-----------|-------------|
| Saliva | 839 | 665 | 611 | 657 | 603 | - | 97 | 96 |
| Anterior_nares | 1126 | 969 | 585 | 299 | 168 | - | 63 | 64 |
| Right_Antecubital_fossa | 1072 | 940 | 539 | 240 | 161 | - | 72 | 73 |
| Left_Retroauricular_cresce | 1330 | 1123 | 860 | 265 | 105 | - | 78 | 73 |
| Left_Antecubital_fossa | 1209 | 1054 | 672 | 261 | 178 | - | 63 | 63 |
| Right_Retroauricular_cresce | 1031 | 875 | 603 | 250 | 97 | 683 | 65 | 64 |
| Palatine_Tonsils | 684 | 444 | 489 | 496 | 376 | - | 86 | 86 |
| Subgingival_plaque | 602 | 219 | 309 | 277 | 257 | 405 | 71 | 63 |
| Throat | 930 | 709 | 724 | 894 | 714 | 778 | 95 | 90 |
| Vaginal_introitus | 500 | 398 | 306 | 173 | 131 | - | 47 | 46 |
| Buccal_mucosa | 617 | 409 | 446 | 333 | 308 | 494 | 77 | 68 |
| Hard_palate | 672 | 385 | 513 | 550 | 414 | 475 | 89 | 89 |
| Supragingival_plaque | 513 | 373 | 262 | 227 | 179 | 327 | 51 | 51 |
| Mid_vagina | 364 | 322 | 188 | 147 | 152 | 247 | 31 | 34 |
| Attached_Keratinized_gingiva | 622 | 273 | 399 | 314 | 383 | 474 | 55 | 53 |
| Posterior_fornix | 268 | 249 | 107 | 117 | 97 | - | 22 | 24 |
| Tongue_dorsum | 516 | 445 | 372 | 376 | 111 | 343 | 76 | 75 |

Table S5. DA results between stool and other body sites based on HMP data at the species level (- means an error occurred). The proportion of zeros ranged from 81% to 90%, the total number of species varied between 243 and 1123. There were some errors occurred when running DESeq2 and edgeR.

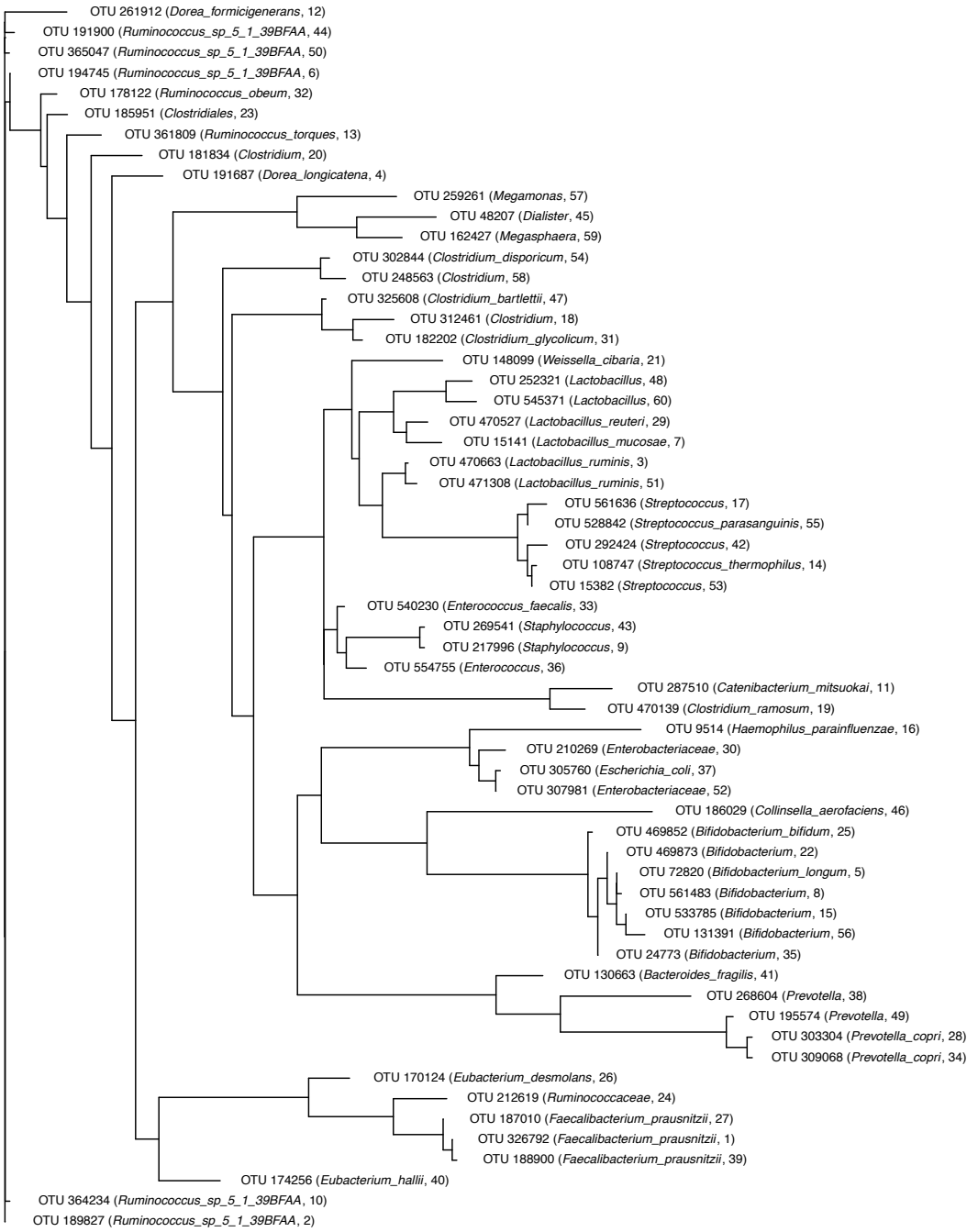


Figure S19. The phylogenetic tree of 60 bacterial taxa inferred by maximum likelihood. The text next to each OTU gives the taxonomic information and the rank of relative importance obtained by applying the random forest algorithm.

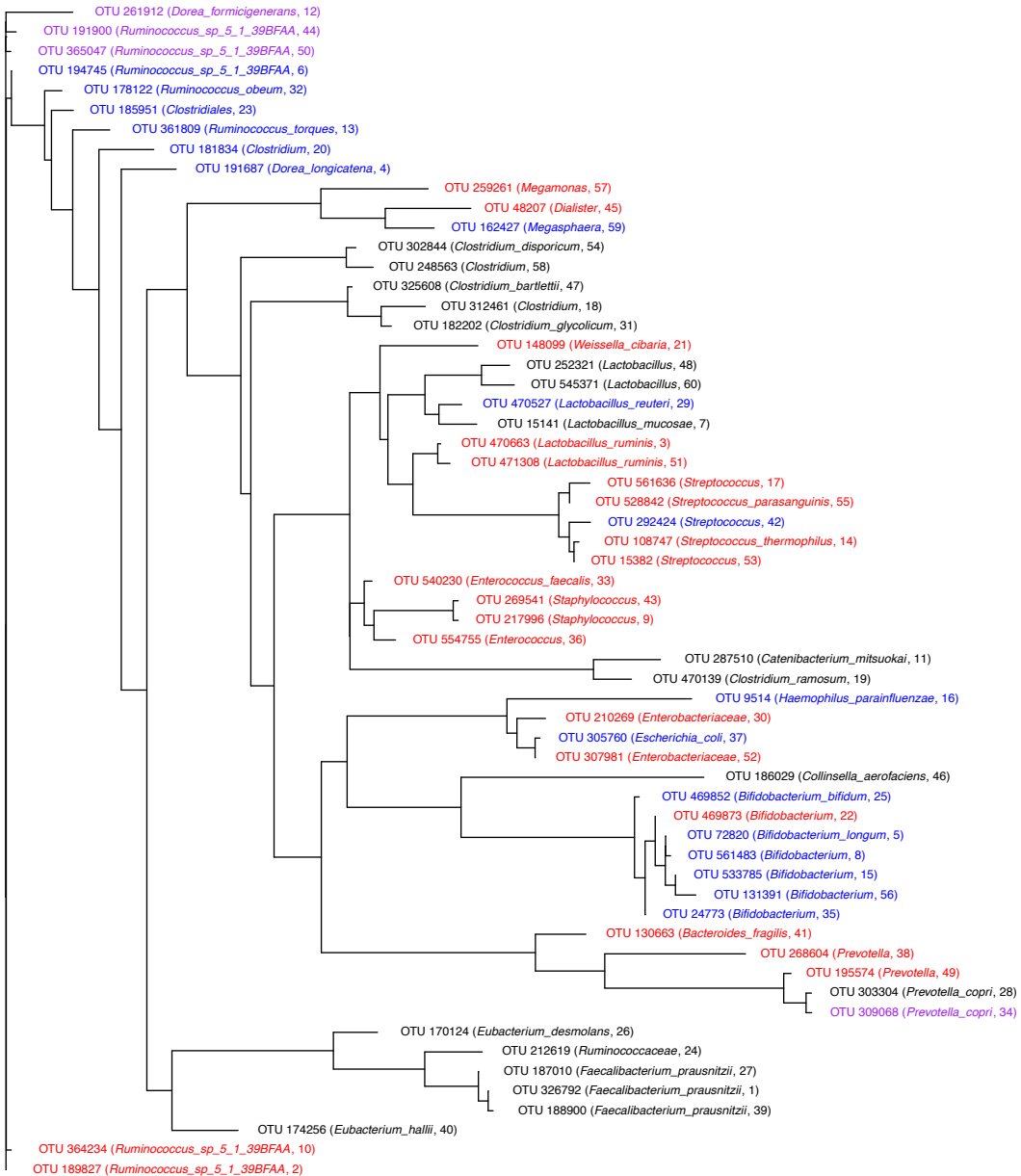


Figure S20. Tree-based visualization of DA testing results. Species detected uniquely by adaANCOM, uniquely by its competitors, and by adaANCOM and one of its competitors, are shown in red, purple, and blue, respectively.